Defects in keratinocyte activation during wound healing in the syndecan-1-deficient mouse

Mary Ann Stepp[1,2,*], Heather E. Gibson[3], Purvi H. Gala[1], Drina D. Sta. Iglesia[1], Ahdeah Pajoohesh-Ganji[1], Sonali Pal-Ghosh[1], Marcus Brown[1], Christopher Aquino[1], Arnold M. Schwartz[4], Olga Goldberger[3], Michael T. Hinkes[3] and Merton Bernfield[3]

[1]Department of Anatomy and Cell Biology, The George Washington University Medical School, Washington DC 20037, USA
[2]Department of Ophthalmology, The George Washington University Medical School, Washington DC 20037, USA
[3]Division of Developmental and Newborn Biology, Department of Pediatrics, Harvard Medical School, Boston, MA 02115, USA
[4]Department of Pathology, The George Washington University Medical School, Washington DC 20037, USA
*Author for correspondence (e-mail: mastepp@gwu.edu)

Accepted 22 August 2002
Journal of Cell Science 115, 4517-4531 © 2002 The Company of Biologists Ltd
doi:10.1242/jcs.00128

Summary

Mice lacking syndecan-1 are viable, fertile and have morphologically normal skin, hair and ocular surface epithelia. While studying the response of these mice to corneal epithelial and skin wounding, we identified defects in epithelial cell proliferation and regulation of integrin expression. mRNA profiling of corneal epithelial tissues obtained from wild-type and syndecan-1$^{-/-}$ mice suggest that these defects result from differences in overall gene transcription. In the cornea, syndecan-1$^{-/-}$ epithelial cells migrate more slowly, show reduced localization of α9 integrin during closure of wounds and fail to increase their proliferation rate 24 hours after wounding. In the skin, we did not document a migration defect after full thickness wounds but did observe cell proliferation delays and reduced localization of α9 integrin in the syndecan-1$^{-/-}$ epidermis after dermabrasion. Despite increased cell proliferation rates in the uninjured syndecan-1$^{-/-}$ epidermis and the corneal epithelium, morphologically normal epithelial thickness is maintained prior to injury; however, wounding is accompanied by prolonged hypoplasia in both tissues. Analyses of integrin protein levels in extracts from full thickness skin, revealed increased levels of α3 and α9 integrins both prior to injury and after hair removal in syndecan-1$^{-/-}$ mice but no increase 2 days after dermabrasion. These data for the first time show involvement of α9 integrin in skin wound healing and demonstrate essential roles for syndecan-1 in mediating cell proliferation and regulation of integrin expression in normal and wounded epithelial tissues.

Key words: Syndecan-1, Wound healing, Cell proliferation, Integrins

Introduction

Syndecans are a family of four heparan sulfate proteoglycans (HSPGs) expressed on all adherent cell surfaces and are known to function as co-receptors for various growth factors and matrix molecules (Perrimon and Bernfield, 2000; Park et al., 2000b; Rapraeger, 2000; Perrimon and Bernfield, 2001; Rapraeger, 2001; Woods, 2001). Syndecan-1 (synd1) is abundant in normal epithelial cells and tissues, localizing to both basal and suprabasal cell layers. Furthermore, synd1 and other HSPGs are known to play roles in wound healing, with gene expression upregulated in response to injury and shed synd1 ectodomain accumulating in the wound fluid, where it is involved in mediating protease activity (Kainulainen, V. et al., 1998; Fitzgerald et al., 2000; Park et al., 2000a). Disruption of synd1 expression in cultured cells leads to an epithelial-mesenchymal transformation, with associated changes in cell polarity, cell-cell adhesion and altered epithelial-specific gene expression (Dobra et al., 2000; Rapraeger, 2001).

Previous studies have shown that the expression and localization of keratinocyte integrins are upregulated in response to both skin (Hertle et al., 1992; Kainulainen, T. et al., 1998) and corneal (Stepp et al., 1996; Stepp and Zhu, 1997) wounding. Integrins within the cell membrane associate with many different molecules, including tetraspanins, growth factor receptors, membrane-associated proteinases and syndecans. These associations can alter integrin function either by clustering signaling molecules, altering integrin internalization and turnover and/or by directly increasing ligand binding. The primary syndecan expressed by keratinocytes is synd1 with lower amounts of syndecan-4 (synd4) also expressed. Since syndecans can act as co-receptors with integrins for matrix molecules, the loss of synd1 could affect integrin-mediated functions.

The heparan sulfate side chains present on syndecan ectodomains associate with growth factors and extracellular matrix molecules. Extracellular growth factor:syndecan associations can either stimulate or inhibit tissue-specific cellular functions depending on the cellular context. Normally syndecans bring growth factors close to the cell surface and increase their association with receptors; however, if syndecan is shed from the cell surface by the action of proteases, the growth factor:syndecan interaction will reduce the concentration of growth factors at the cell surface. Shed syndecan ectodomains are found in the wound fluid after skin wounding (Park et al., 2000a), and the shedding of synd1 and synd4 has recently been demonstrated to be regulated by the

action of TIMP-3-specific metalloproteinases (Fitzgerald et al., 2000). The most extensively studied syndecan:growth factor associations are those involving fibroblast growth factor (Filla et al., 1998; Kusano et al., 2000) and hepatocyte growth factor (Cornelison et al., 2001; Derksen et al., 2002). Although the integrin-syndecan interaction has been suggested by several studies (Couchman and Woods, 1999; Saoncella et al., 1999; Kusano et al., 2000), direct association between synd1 and integrin has not been demonstrated. Syndecans can also interact with proteins of the ADAMs (a disintegrin and metalloproteinase) family; the ADAM-12–syndecan interaction leads to integrin activation and cell adhesion (Iba et al., 2000).

Others have studied the roles played by the cytoplasmic domain of the syndecan core protein (Grootjans et al., 1997; Hsueh and Sheng, 1999; Grootjans et al., 2000; Hsueh et al., 2000). All four syndecan family members have cytoplasmic tails that contain binding motifs of the PDZ type. PDZ domains, named after the first three protein families shown to contain these motifs – the PSD-95, Disc-large (dlg) and Zonula occludens – are known to organize protein complexes at the cytoplasmic face of the cell membrane and to mediate the interaction of the actin cytoskeleton with these complexes.

The dogma that heavily modified core proteins, including syndecans and other HSPGs, are functional exclusively outside cells is beginning to be questioned. It is clear that cells expressing synd1, including epidermal and corneal keratinocytes, retain most of their synd1 within intracellular compartments. The retention of large heavily glycosylated proteins and proteoglycans was once believed to be due to their long transit time through the endoplasmic reticulum and Golgi apparatus, but several lines of evidence suggest intracellular functions. Brockstedt and colleagues have begun to look at the role of synd1 in tubulin-mediated events (Brockstedt et al., 2002), including stabilization of the mitotic spindle and tubulin-mediated transport of growth factors to the nucleus. The mechanism whereby synd1 mediates transport within the cytoplasm probably involves transmembrane and cytoplasmic domain sequences that remain available to cytosolic adaptors and docking proteins after endocytic vesicles have budded off from the ER to make their way to the plasma membrane. The cytoplasmic and transmembrane domains of synd1 have been shown recently to mediate a non-coated pit endocytic pathway involving detergent-insoluble rafts (Fuki et al., 2000). The kinetics of the synd1-mediated pathway are rapid, with a $t_{1/2}$ of 1 hour and requiring intact actin microfilaments and active tyrosine kinases. Detergent-insoluble rafts mediate integration of signal transduction by growth factor receptors and integrins after activation (Zajchowski and Robbins, 2002). The idea that rafts might also regulate endocytic traffic, in part, via synd1-mediated events, is interesting and requires further study. The absence of synd1 might well affect the overall ability of cells to regulate raft-mediated signal integration, which is essential for the propagation of α6β4-integrin-mediated signals (Mainiero et al., 1997; Mariotti et al., 2001).

Using our knowledge of the synd1 mouse gene (Hinkes et al., 1993), we designed a targeting vector to disrupt the expression of synd1 in mice. Given the abundance of synd1 on stratified epithelia and the known roles syndecans play in cell migration, we postulated that the loss of synd1 from the surface of corneal and skin epithelial cells would affect the ability of these tissues to respond to injury. Syndecan-1-knockout (synd1ko) mice appear healthy and otherwise normal; however, when we studied the ability of these mice to heal wounds, we observed healing defects after both corneal and skin wounding. To begin to determine the mechanism behind the healing defects, additional in vivo experiments were performed to assess cell proliferation, barrier function and the localization and expression of several molecules implicated in epithelial cell migration. In addition, mRNA expression profiles of unwounded and wounded wild-type (wt) and synd1ko keratinocytes were assessed in the cornea.

Additional studies using synd1ko mice have shown synd1 mediates Wnt-1-induced mammary tumor progression (Alexander et al., 2000), resistance to bacterially mediated lung infections (Park et al., 2001), leukocyte adhesion to endothelia (Gotte et al., 2002) and increased susceptibility to growth-factor-induced angiogenesis (Gotte et al., 2002). This report is the first providing a description of the generation of synd1ko mice and defects present within their epithelial tissues. A previous report showed skin wound healing and cell migration defects in the syndecan-4 knockout (synd4ko) mouse (Echtermeyer et al., 2001). Although healing problems in the synd4ko mouse appear to result primarily from defects in fibroblast migration, results presented in this study show that the delayed healing in the synd1ko mouse results from impaired functioning of keratinocytes.

Materials and Methods

Materials and chemicals

The majority of chemicals used in these studies were obtained from Sigma Chemical Co. (St. Louis, MO), including ethylene glycol aminoethyl ether tetraacetic acid, bovine serum albumin (BSA), sodium dodecyl sulfate (SDS) and horse serum. Ketamine was purchased from Fort Dodge Veterinary Supplies (Fort Dodge, IA), xylazine from Vedco (St. Joseph, MO) and sodium pentobarbital from Veterinary Laboratories, Inc. (Lenexa, KS). Tissue Tek II OCT compound was obtained from Lab Tek (Naperville, IL), and proparacain eye drops and erythromycin ophthalmic ointment were obtained from Baush & Lomb (Tampa, FL). We purchased coverslips and paraformaldehyde from Fisher Scientific (Somerville, NJ). Slides were obtained from Shandon (Pittsburgh, PA), pap pen from Electron Microscopy Sciences (Washington, PA) and anti-fade mounting media from Vector Labs (Burlingame, CA). All images were printed on a Tektronix (Dallas, TX) laser 450 DS printer.

Construction of the synd1-targeting vector and generation of synd1-deficient mice

The mouse synd1 gene structure was described previously (Hinkes et al., 1993). The targeting vector used was a 7.1 kb *Mbo*I/*Sal*I fragment isolated from a mouse 129 synd1 genomic DNA fragment containing DNA homologous to the endogenous gene that included 1.4 kb of the 5′ flanking sequence, the entire 0.3 kb of the first exon and 5.3 kb of the large first intron. A PKG neo-positive selection marker was inserted into a unique restriction site to disrupt the signal peptide sequence, making it unlikely that the mature proteins would reach the cell surface. A negative selection marker, MC1 thymidine kinase, flanked the first intron sequences at the 3′ end of the construct.

The linearized targeting vector was transfected by electroporation into J1 mouse 129 embryonic stem (ES) cells (Li et al., 1992). A positive-negative selection strategy using G418 and gancyclovir was employed, and ES cell colonies were evaluated for homologous recombination by Southern blot analysis (Thomas and Capechi, 1987). Following karyotype analysis, one of the targeted ES cell

clones (1G7) was microinjected into C57B1/6 and BALB/c blastocysts. Chimeric mice were maintained, and subsequently the synd1 mutation appeared in the germ line. Breeding of the heterozygous offspring resulted in animals homozygous for the synd1-targeted mutation. ES cell clones and mice were genotyped by standard Southern blot techniques (Laird et al., 1991) using *Bst*EII digests of genomic DNA and a 760 bp synd1 genomic probe that is external to the targeting construct and located in the first intron. This probe identifies a 7.1 kb fragment from the endogenous allele and a 8.6 kb fragment from the PGK neo-containing targeted allele.

The expression of synd1 and synd4 mRNAs in synd1ko and wild-type mouse skin was assessed by northern blots as described previously (Kim et al., 1994). 10 μg each of total RNA obtained from adult synd1ko and wild-type mouse skin were run on a 1% formaldehyde gel and blotted onto nitrocellulose membranes, using a vacuum blotter. Probes for northern blots comprised cDNAs encoding the ectodomains of synd1 and synd4 labeled with P^{32} dNTPs, using the Rediprime II Kit (Amersham Pharmacia; Piscataway, NJ) and were labeled to a specific activity equal to or greater than 6×10^8 cpm/μg. Blots were hybridized using Rapid-Hyb hybridization solution (Amersham Pharmacia; Piscataway, NJ) for 1 hour at 68°C and were then washed twice in 2×SSC-0.1% SDS at room temperature, and once in 0.1×SSC with 0.1% SDS at 60°C for 30 minutes. Blots were exposed overnight.

Animal protocols

For full-thickness skin wound-healing experiments, mice were anaesthetized with Avertin, and two full-thickness, 3 mm diameter wounds were made using a sterile biopsy punch on the shaved and disinfected backs of 25 synd1ko and 25 wild-type mice, at 4-6 weeks of age. Wounds were left undressed, and all mice were housed separately after wounding. At various times after wounding, mice were sacrificed using a Metofane anesthetic overdose, and wounds with a 1 cm unwounded skin border were harvested and processed for histochemistry. The time points analyzed included 2, 3, 4, 5 and 9 days post-injury.

For dermabrasion experiments, the procedure described by Wojcik and colleagues was followed (Wojcik et al., 2000). 10 synd1ko and 10 wt mice between 7-9 weeks-of-age were anaesthetized and the fur on their backs trimmed with scissors and removed using depilatory cream (Nair creme depilatory; 1 minute, Carter-Wallace Inc., New York, NY). Skin was disinfected and allowed to dry. Cellophane tape (Scotch brand; 0.5 in width) was then applied and removed quickly eight times centrally on the backs of mice. Dermabraded areas were treated with Betadine solution and allowed to recover for either 2 or 5 days. Two hours prior to sacrifice, mice were injected with BrdU solution; after sacrifice by anaesthetic overdose, full-thickness skin tissues were dissected free from underlying fascia, rapidly frozen in liquid nitrogen and processed for either immunofluorescence or immunoblotting. For immunofluorescence, the frozen skin tissues were trimmed to approximately 1 cm^2 and then embedded in tissue-embedding medium. For Western blotting, frozen skin tissues were ground to a fine powder using a mortar and pestle kept frozen with liquid nitrogen. Powdered skin was extracted as described previously (Stepp et al., 1996). For immunoblotting, control tissues were of two types: skin taken from mice whose hair had been removed immediately after sacrifice (control) and skin taken from mice whose fur had been removed 2 days prior to sacrifice but whose skin had not been subjected to dermabrasion (unwounded). For wounded tissues, 2 mm areas of skin tissue surrounding the involved skin were obtained.

All corneal wound healing experiments on mice were conducted in compliance with the recommendations of the Association for Research in Vision and Ophthalmology. Manual debridement wounds were created on the corneas of 8-week-old synd1ko and wild-type mice, as described previously (Stepp and Zhu, 1997). Mice were anaesthetized with general anesthesia and their eyes numbed with a topical anesthetic. Corneas were then scraped with a dull scalpel to remove the epithelium within a 1.5-mm central corneal area, which had been demarcated with a dull trephine. Animals were sacrificed by lethal overdose at times ranging from 12 hours to 12 weeks. To determine the timing of wound closure, corneas were stained with a vital dye at various times after wounding, then evaluated under the dissecting microscope and determined to be ‘opened’ or ‘closed’ on the basis of whether the dye had stained the central cornea. The numbers of animals used per time point for wound closure analyses were as follows: 12 hours: (7 wildtype and 6 synd1ko), 18 hours (10 wildtype and 17 synd1ko), 24 hours (14 wildtype and 25 synd1ko), 36 hours (8 wildtype and 16 synd1ko), 48 hours (no wildtype and 13 synd1ko), and 60 hours (no wildtype and 4 synd1ko). Data were analyzed for statistical significance using the Mantel-Haenszel Chi-Square Test. After the eyes were assessed under the dissecting microscope for scarring and neovascularization, they were enucleated and frozen in Tissue Tek II OCT compound for immunofluorescence and confocal microscopy. For both whole mount and cryostat-sectioned immunofluorescence studies, at least three eyes from three different animals were used per time point.

For mRNA profiling, after sacrifice, corneal epithelial sheets were harvested from unwounded mice and from mice at 18 hours after wounding, by scraping and immediate freezing in liquid nitrogen. The debrided epithelia from no fewer than 20-25 unwounded and 15-20 wounded corneas were pooled to obtain sufficient RNA for RNA profiling. Frozen tissues were used to extract RNA for cDNA array analyses using the Atlas 1.2 mouse cDNA array (Clontech; Palo Alto, CA). Comparisons were made between unwounded and wounded wild-type RNAs, between unwounded wild-type and unwounded synd1ko RNAs, and between unwounded synd1 and wounded synd1 RNAs using Atlas Image 1.0 (Clontech; Palo Alto, CA).

To determine the barrier function of the corneal epithelium after wounding in the synd1ko mice, a surface biotinylation procedure was used (Xu et al., 2000). Wt and synd1ko mice were wounded and allowed to heal for 4 weeks. After sacrifice, eyes were removed and placed in 1 mg/ml sulfo-NHS-LC-biotin (Pierce Chemical, Rockford, IL) in Hank’s media supplemented with 1 mM $CaCl_2$ and 2 mM $MgCl_2$. After 30 minutes at room temperature, tissues were rinsed in PBS and frozen in OCT for sectioning. To determine the extent of penetration of biotin, tissue sections were incubated with rhodamine-avidin (Vector Labs, Burlingame, CA) for 1 hour and slides coverslipped and viewed using the confocal microscope. To visualize Zonula occludens (ZO-1) localization and biotin penetration simultaneously, tissues were incubated first in primary antibody alone followed by Alexa Fluor 488 (Molecular Probes, Eugene, OR) conjugated secondary antibody and rhodamine-avidin.

Immunohistochemical studies

Corneal or skin tissues were sectioned (8 μm), and unfixed frozen sections used for immunofluorescence microscopy as described previously (Stepp and Zhu, 1997). Synd1 localization was evaluated using a rat monoclonal antibody against the synd1 core protein (281-2, now commercially available from Pharmingen, cat # 09341D; San Diego, CA) and the synd4 core protein. Polyclonal anti-peptide sera recognizing α9 and β4 integrins were characterized as described previously (Sta. Iglesia et al., 2000). The rat monoclonal against ZO-1 was obtained from Chemicon (cat # MAB1520; Temecula, CA). Secondary antibodies were obtained from Molecular Probes (Eugene, OR); Alexa Fluor 488 and/or Alexa Fluor 568 were used for double labeling experiments.

Whole mounts were performed on eyes that were fixed immediately after sacrifice in 70% methanol/DMSO for 2 hours followed by 100% methanol overnight (as a minimum length of time). After fixation, corneas were dissected away from the back of the eye, rehydrated, blocked and processed for α9 integrins. After the final wash after the

secondary antibody, tissues were processed for with propidium iodine prior to mounting en face, for viewing via confocal microscopy. Images were viewed and captured by confocal scanning laser microscopy using an inverted Olympus BX60 fluorescence microscope (OPELCO, Dulles, VA) equipped with the Biorad MRC 1024ES laser system, Version 3.2 (Bio-rad, Hercules, CA). All images were imported into Adobe Photoshop 5.0 (Adobe Systems; Palo Alto, CA).

Bromodeoxyuridine (BrdU) cell proliferation analyses

Cell proliferation was assessed using the BrdU Labeling and Detection Kit I (Roche Diagnostics; Indianapolis, IN), as recommended by the manufacturer. Corneas were wounded as described above, and after sacrifice, eyes were immediately placed in a BrdU-containing labeling solution consisting of complete MEM (Stepp et al., 1997). After 30 minutes in labeling solution, the eyes were washed three times and allowed to incubate for an additional 15 minutes in MEM without BrdU.

For dermabrasion studies, skin was obtained from mice injected with BrdU 2 hours prior to sacrifice. Uninvolved and involved skin was removed from the backs of the mice, gently stretched and flattened on a glass surface and rapidly frozen with liquid nitrogen. For corneal studies, intact eyes, and for skin studies, 1-2 cm^2 pieces of skin were embedded in OCT and 8 μm sections cut. Sections were hydrated and fixed in ice-cold 70% methanol in 50 mM glycine buffer, pH-2, for 20 minutes at –20°C. After fixation, sections were incubated in PBS twice for 2 minutes each, incubated with 2.5% trypsin in 0.1% $CaCl_2$ in PBS for 3 minutes at room temperature, briefly washed in PBS and then transferred to a solution containing 4 M HCl for 3 minutes at room temperature. Sections were washed again twice for 5 minutes each in PBS and then transferred to blocking solution (1% BSA and 0.1% horse serum in PBS). Slides were then processed for immunofluorescence. To quantify proliferation rates after corneal wounding, the numbers of labeled cells per unit area of the basal membrane surface of the basal cells were determined using morphometry. No fewer than five visual fields were counted per time point. At least two corneas from two different experimental procedures and two slides for each time point studied were used for these studies. For skin, the numbers of labeled cells per visual field at 20× magnification were assessed. Five wild-type and five synd1ko mice were assessed for data obtained 2 days after dermabrasion; two wild-type and two synd1ko mice were used for data obtained 5 days after wounding. The numbers of labeled cells in at least three different sections from each mouse were counted. Data were analyzed for significance using the unpaired *t*-test.

Results

Syndecan-1-deficient mice show no embryonic lethality and develop and reproduce normally

Genomic clones encoding the murine *synd1* gene were targeted in strain 129 ES cells, with a construct containing a 7.0 kb fragment of DNA sequence interrupted in exon 1 by a neomycin resistance cassette driven by a PGK promoter (Fig. 1A). Following electroporation of the vector, positive-negative selection was used to isolate targeted clones, and homologous recombination was detected by Southern blot in 14 of 126 clones. ES cells with a normal karyotype derived from a single clone were injected into C57BL/6 and BALB/c blastocysts, which were then placed into pseudopregnant dams. Chimeras were identified by coat color, and germline transmission of the disrupted allele was observed in both C57BL/6 and BALB/c mice. Crosses of $synd1^{+/-}$ heterozygous parents resulted in mice homozygous for the mutant *synd1* gene (Fig. 1B). To establish that both synd1 alleles had been disrupted, the level of synd1 mRNA was assessed by northern blot analysis (Fig. 1C). The synd1ko mice lacked synd1 mRNA, whereas synd4 mRNA was present in equal amounts in both synd1ko and wt mice.

The progeny resulting from n=23 matings of heterozygous parents from either C57BL/6 or BALB/c lines showed a Mendelian transmission pattern, with 24% homozygotes, 46% heterozygotes and 30% wildtype, suggesting that the disruption of the *synd1* gene does not alter mouse viability or cause embryonic lethality. Reproductive capacity was unchanged, as no significant difference in litter size was observed between matings of homozygous-null and wild-type mice of both C57BL/6 and BALB/c strains. No histological differences between tissues of the synd1ko and wild-type mice were observed at either 6 weeks or 6 months of age. Routine serum chemistry and hematologic studies revealed no differences between wild-type and synd1ko mice.

The characteristics of synd1ko epidermis and corneal epithelia were assessed by immunofluorescence (Fig. 1D). In wild-type skin and cornea, synd1 was most abundant within the cytoplasm at perinuclear locations as well as at cell-cell membranes. It was not present at the apical squames or at the basal cell basement membrane zone. β4 integrin, a component of the hemidesmosomes, was present primarily at the basal cell basal membranes in both the wt and the synd1ko cornea and skin. Synd1, as expected, was absent from the skin and cornea of the synd1ko mice. Despite the presence of synd4 mRNA in wild-type and synd1ko mouse skin, synd4 protein was below detection in both wild-type and synd1ko skin and cornea, and was not upregulated in synd1ko epithelia (data not shown). The epithelial integrins α3 and α9, as well as E-cadherin and ZO-1, were also assessed in the skin and cornea of the wild-type and synd1ko mice and were found to be localized to the expected sites in the synd1ko mouse tissues. Although β4 integrin localized to the basement membrane zone, ZO-1 was most abundant at the apical-surface of stratified epithelia. α3 and α9 integrins were localized to the apical, lateral and basal cell membranes of basal keratinocytes in skin. α9 integrin localization in the cornea was restricted to the limbal basal cells, whereas α3 integrin was expressed equally in the limbus and central cornea. The similarity between these wild-type and synd1ko epithelial tissues in terms of localization of markers for epithelial tissue polarity indicated that the synd1ko tissues are normal.

Synd1ko mice do not re-epithelialize corneal wounds properly

Synd1 is highly regulated during the repair of skin wounds, with expression increasing in both the epidermis and dermis, and shed ectodomain accumulating in the granulation tissues and wound fluid (Bernfield et al., 1999). To determine whether the synd1ko mouse epithelial tissues can repair wounds normally, we first used a corneal epithelial debridement model, which involves the manual removal of a circular patch of epithelial cells at the center of the cornea, leaving the underlying basement membrane zone intact and native (Fujikawa et al., 1984; Gipson et al., 1984). Corneal debridement wounds in the synd1ko mice re-epithelialized at a slower rate than those in the wildtype, with differences becoming statistically significant

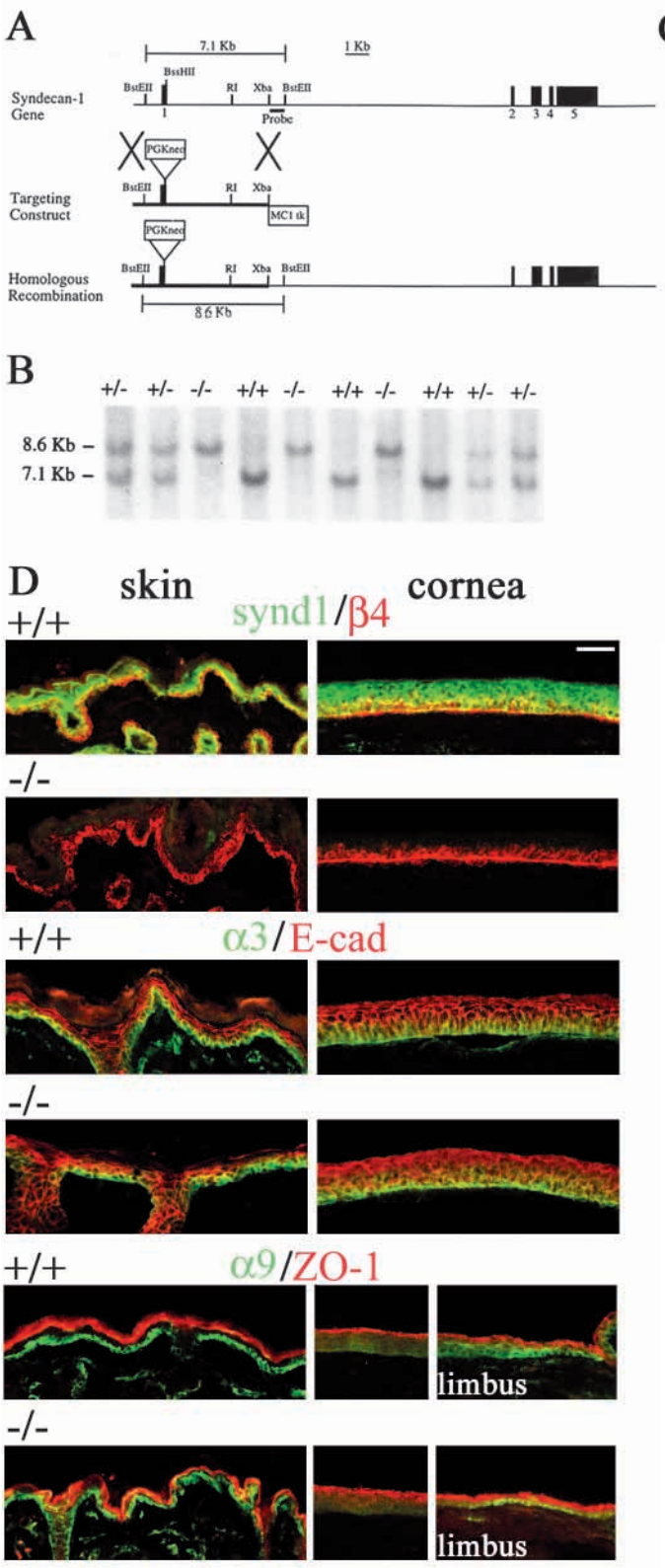

Fig. 1. Synd1ko mice express no synd1 mRNA or protein, and their epithelial tissues appear normal. (A) The targeting vector was a *Mbo*I/*Sal*I fragment with homology to the endogenous gene and includes 1.4 kb of the 5′ flanking sequence, the entire 0.3 kb first exon and 5.3 kb of the first large intron. Positive (PGK neo) and negative (MC1-tk) selection markers were used. The disrupted allele was 8.6 kb versus the wild-type allele, which was 7.1 kb. (B) Using a 3′ probe, Southern blot analyses of tail DNA isolated from two litters of mice included wildtypes ($^{+/+}$), heterozygotes ($^{+/-}$) and homozygotes ($^{-/-}$) for the disrupted gene. (C) Northern blots show that, when equal amounts of RNA isolated from wild-type and $^{-/-}$ mouse skin are run out on gels and transferred to nitrocellulose, the synd1ko mice have no detectable synd1 mRNA, whereas the wild-type mice do. Replicate blots probed with a synd4 cDNA, serving as a positive control for RNA quality, confirm the presence of synd4 mRNA in both wild-type and $^{-/-}$ tissues, but there is no upregulation in the synd1ko tissues. RNA sizes are indicated on the right; synd1 mRNA is present as two discrete bands of 2.6 and 3.4 kb, whereas synd4 mRNA is 2.6 kb. (D) Using confocal microscopy, skin and corneal tissues from wild-type and synd1ko mice were evaluated to determine the degree of colocalization of synd1 and β4 integrin, α3 integrin and E-cadherin or α9 integrin and ZO-1. Merged images are presented. Although E-cadherin is expressed at the lateral membranes of basal cells, it is less abundant at this site, and the large amount of α3 integrin in basal cells makes it difficult to document E-cadherin–α3-integrin co-expression in the basal cells in these merged images. For the α9/Z0-1 merged images of the corneal limbal region, the central cornea is located to the left and the conjunctiva is to the right. No differences in the localization of integrins, E-cadherin or ZO-1 between wild-type and synd1ko tissues are observed. Bar in D, 90 μm.

(P<0.05) by 24 hours after wounding (Fig. 2A,B). Data showed that, whereas 50% of the corneal wounds were closed at 22 hours in the wild-type mice, it took 30 hours for 50% of the synd1ko wounds to close. Routine histology was performed to assess the morphology of the corneal epithelial cells after wounding (Fig. 2D). During migration, the leading edge extended normally in both wild-type and synd1ko mice; however, there appeared to be more inflammatory cells beneath the leading edge in the healing synd1ko corneas. Although the wild-type corneas appeared morphologically normal 1 week after wounding, at 2 weeks, the epithelium of the synd1ko corneas showed evidence of hypoplasia.

Cell proliferation abnormalities are present in the synd1ko corneal epithelial cells before and after wounding

To determine whether there were differences between cell proliferation in the synd1ko and wild-type corneal epithelial cells, cell proliferation was assessed using BrdU (Fig. 2C). Surprisingly, the synd1ko corneal epithelial cells showed a higher cell proliferation rate prior to wounding than did the wild-type cells. For wild-type mice, the proliferation rate was significantly elevated 24 hours after injury, when the majority

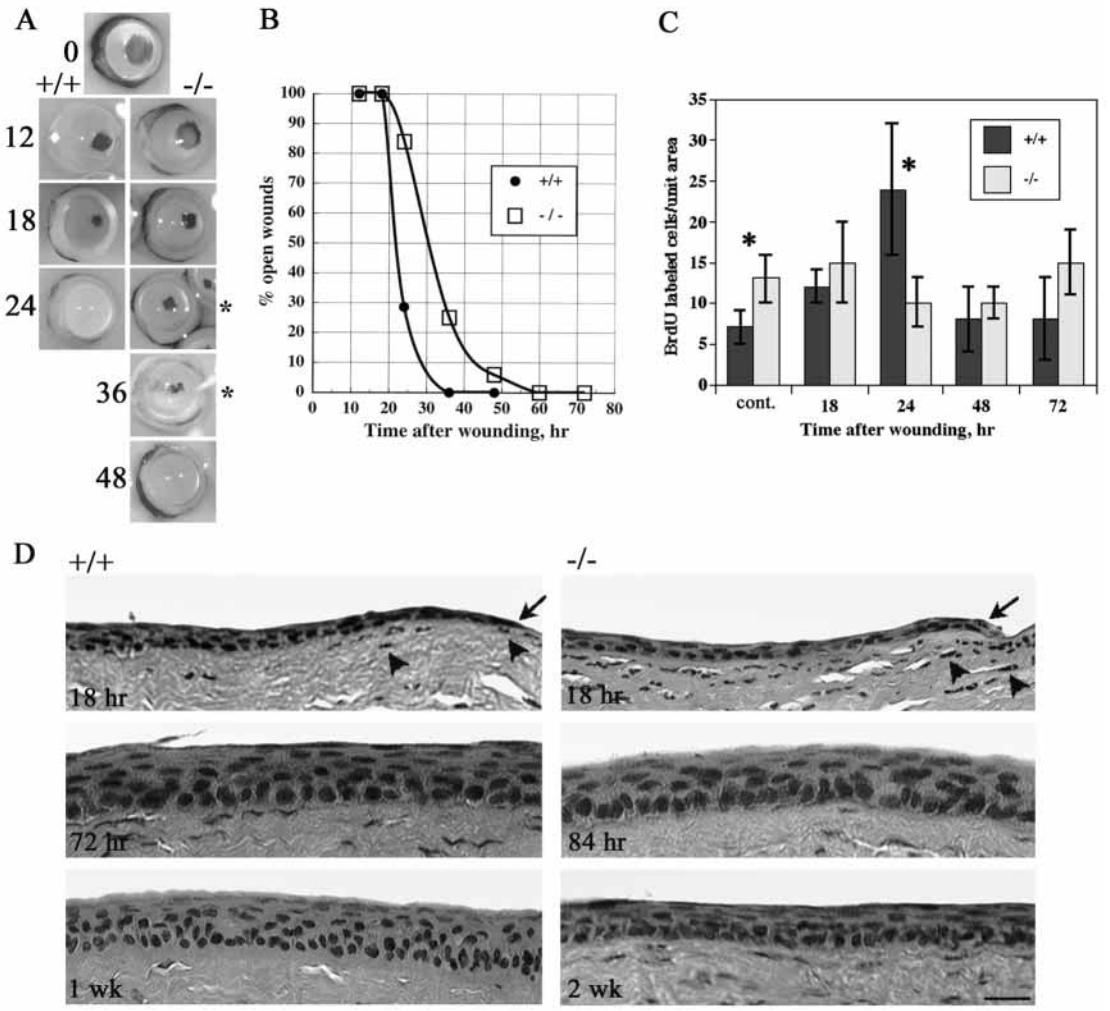

Fig. 2. The absence of synd1 leads to delayed closure of corneal epithelial scrape wounds, which is associated with a failure to increase cell proliferation after wounding. The numbers of open wounds and corneas used to generate these data are presented in the methods section. (A) Representative photomicrographs obtained after wounding at the indicated times (d, day) are depicted. The delay in closure of epithelial wounds is statistically significant ($P<0.05$) at 24 and 36 hours (asterisk) as determined using the Mantel-Haenszel Chi-Squared test. (B) Data from the experiment described in A were used to create a graph showing the time (hr, hour) of 50% wound closure. There is an 8-hour delay in the 50% wound closure time in synd1ko mice compared with wild-type mice. (C) Cell proliferation was assessed using BrdU. Data show that, although wild-type corneal epithelial cells increase proliferation at 24 hours after wounding, the synd1ko animals fail to respond to the corneal wound by increasing their proliferation rate at any time point analyzed. Data for the synd1ko are significantly ($P<0.05$) different from wildtype at 24 hours. Surprisingly, there is also a significant ($P<0.05$) increase in proliferation rate in the unwounded synd1ko mice compared with that in unwounded wild-type mice. Data are compared using the unpaired *t*-test, and asterisks indicate significant differences between groups. (D) Histology shows that migration in the synd1ko mouse cornea is associated with a transient increase in inflammatory cells in the corneal stroma and a failure to restratify properly by 2 weeks. 18 hours after wounding, more inflammatory cells are observed beneath the migrating synd1ko epithelial sheet than in the wildtype. Arrows indicate the leading edge, and the arrowheads indicate inflammatory cells; direction of cell migration is from left to right. Bar, 60 μm.

of the wounds were closed; by 48 hours, the proliferation rate was back to that observed in unwounded wild-type corneas. Although the rate of proliferation in the syn1ko corneas was higher before wounding, it did not increase significantly at any time after wounding. Thus, the cellular signal required to trigger increased cell proliferation after wounding was either not transmitted or not recognized in corneal epithelial cells in the absence of synd1.

Proliferation rate differences among cells generally reflect differences in steady-state mRNA levels. To determine if there were any overall differences in steady-state mRNA levels, mRNA profiling was performed using a mouse cDNA array on total RNA isolated from both unwounded and wounded wild-type and synd1ko epithelial tissues (Table 1). mRNA was extracted from corneal epithelial tissues obtained by manual debridement of the ocular surface of unwounded mice immediately after sacrifice or mice at 18 hours after wounding – a time when the majority of epithelial cells were still migrating but prior to the onset of wound-induced cell proliferation in wt corneas. Only mRNAs whose expression varied three-fold or greater are listed in Table 1. Several differences between mRNAs expressed in unwounded synd1ko

and wild-type corneal epithelia were observed, including mRNAs that encoded proteins important in cell signaling and transcriptional regulation (Table 1A). These differences probably underlie the increase in cell proliferation observed in the unwounded synd1ko corneal epithelial cells. In wild-type corneal epithelial cells, wounding resulted in a three-fold or greater induction of six mRNAs, some of which encoded proteins implicated in cell signaling and migration, such as α6 integrin. There was also a reduction in expression of four mRNAs (Table 1B). During migration, only one mRNA, which encodes keratin 14, normally upregulated in wild-type epithelial cells, was also upregulated in synd1ko epithelial cells. By comparison, six mRNAs were upregulated in wild-type corneas, while only three mRNAs were detected at levels three-fold or greater during migration in extracts from the synd1ko corneas, with nine mRNAs found at levels at least three-fold lower (Table 1C). Among those mRNAs, whose expression was reduced in the synd1ko corneal epithelial cells, were several whose proteins are involved in regulation of gene transcription. Taken together, the mRNA profiling data and the lack of an increase in cell proliferation in synd1ko epithelial tissues after wounding indicate that synd1ko corneal epithelial cells fail to activate appropriately after wounding. The altered expression of several mRNAs prior to injury further suggests that the lack of the synd1 HSPG alters cellular homeostasis and results in the elevated cell proliferation rate observed in quiescent synd1ko corneal epithelial cells.

Table 1. mRNA profiling data

A. Unwounded synd1ko/unwounded wildtype

mRNAs	Variation in expression
58 kDa inhibitor of RNA-activated protein kinase	3
Syndecan-1	–45
STAT-1	–6
Apolipoprotein E	–5
Phospholipase A2	–4
Glutathione-S-transferase5/GST-mu	–3

B. Wounded wildtype/unwounded wildtype

mRNAs	Variation in expression
Keratin 14	10
Early growth response protein	6
c-myc	6
α6 integrin	4
Keratin 19	3
Cathepsin L precursor	3
Endothelial pas domain protein 1	–7
Glutathione-S-transferase5/GST-mu	–5
34/67 kDa Laminin receptor/40s ribosomal protein SA	–3
Protease nexin-II	–3

C. Wounded synd1ko/unwounded synd1ko

mRNAs	Variation in expression
Keratin 14	5
Phospholipase A2	3
Ornithine decarboxylase	3
PAX-6	–4
High-affinity glutamate transporter	–4
Fos-related antigen-2	–4
CD44 antigen precursor/Hermes antigen/HUTCH1	–4
CaCCC box binding protein BKLF	–3
D-box binding protein	–3
Semaphorin B	–3
T-cell death associated protein 51 2.6x	–3
Interferon regulatory factor (IRF1)	–3

Values shown were obtained from analysis of total RNA isolated from four different variables (unwounded wildtype, wounded wildtype, unwounded synd1ko and wounded synd1ko), which were used for analysis of mRNA profiles as described in the methods section. Only mRNAs, which were expressed differentially at levels above three-fold as determined by AtlasImage are shown. Negative numbers indicate that a gene is downregulated.

Transient differences in the localization of α9 integrin are observed immediately prior to wound closure in the cornea

To begin to determine the specific proteins responsible for delayed cell migration in the synd1ko mice, the localization of a number of proteins implicated in cell migration and/or epithelial cell-cell adhesion were evaluated during and after re-epithelialization, when the tissue normally restratifies and the cells repolarize. The proteins evaluated include: cytoskeletal proteins (actin, vinculin, talin, and α-actinin); integrins (α2, α3, α4, α5, α6, α9, αv, β1, and β4); molecules involved in mediating cell-cell adhesion (E-cadherin, ZO-1, occludin, and connexin 43); and matrix proteins including tenascin, laminin-5, perlecan, and entactin.

The localization of α6β4 integrin and synd1 has been reported to be altered during corneal and skin wound healing (Hertle et al., 1992; Stepp et al., 1996; Kainulainen, T. et al., 1998). In our wild-type corneas, synd1 and β4 integrin localization overlapped within basal cells (Fig. 3A). Synd1 in wild-type corneas was expressed in multiple cell layers but was absent from the apical squames. Upon wounding, β4 integrin was no longer polarized exclusively to the basal cell membranes of basal cells but was found instead at lateral and apical membranes and away from the leading edge, at suprabasal cell locations. Although both β4 integrin and synd1 were excluded from the tip of the leading edge, synd1 was present a short distance back from the leading edge, proving that shedding of synd1 into the wound site was restricted to the first few cells at the leading edge after corneal debridement wounding.

In the synd1ko mouse corneas, the localization of β4 integrin was also polarized at the basal cell layer and enhanced at basal membranes (Fig. 3A). After wounding, the changes in β4 integrin localization observed in the synd1ko corneas were identical to those seen in wild-type mice; the timing of the shift in localization of β4 integrin from basal to more lateral cell membranes was also similar. Previously, we and others have shown that the shift of β4 integrin from exclusively basal to basal and suprabasal cells was associated with the loss of hemidesmosomes at the basal cell membranes (Sta. Iglesia and Stepp, 2000).

Although no differences in the localization of β4 integrin were observed before, during or after migration, differences in cellular organization and α9 integrin were seen in en face views of whole mounts of corneal tissues immediately prior to wound closure (Fig. 3B). Unwounded wild-type corneas had no α9 integrin within the cornea but brightly labeled cells were present at the limbal region. A similar pattern was observed for α9 integrin in unwounded synd1ko corneas. When wounds were matched not by time after wounding but for similar sizes

of remaining wound bed, it became apparent that wild-type corneal epithelial cells expressed more α9 integrin in and around the leading edges and at sites where the margins of the epithelial sheets merged (Fig. 3B). In addition, the propidium-iodide-stained nuclei are larger than those of the wildtype, suggesting that the cells are flatter and more spread out in the synd1ko cornea compared to the wildtype. Twelve hours after wounding, α9 integrin was not observed in the epithelial cells of the migrating sheet, and by 48 hours, α9 integrin localization in the central cornea had decreased to background levels in the cornea in both wild-type and synd1ko corneas (data not shown). Other than these differences in α9 integrin localization immediately prior to wound closure, no differences in the localization of other integrins (α2, α3, α4, α5, αv and β1), cytoskeletal proteins (actin, vinculin, talin, and α-actinin), E-cadherin or matrix proteins (tenascin, laminin-5, perlecan, and entactin) accompanied the delayed re-epithelialization rate in the synd1ko mouse corneas.

Defects persist in synd1ko corneas after injury

To determine whether corneal healing defects were transient or persistent, we assessed the localization of β4 and α9 integrins at times up to 12 weeks after wounding by double labeling using an antibody against ZO-1 to indicate the apical-most cell layers. Typical data for tissues obtained 12 weeks after wounding are shown in Fig. 4A. Age-matched unwounded corneas were included in the analyses to control for the possibility of age-related defects in the synd1ko mice. The localization of α9 integrin at the limbal region was not affected in the synd1ko mouse by aging or wounding. Aging in the wild-type and synd1ko corneas resulted in an increase in α9 integrin within numerous corneal basal cells that appears to be independent of wounding. β4 integrin remained polarized to the basal aspect of the corneal epithelial basal cells in the wounded synd1ko mice. The localization of ZO-1 was polarized to the apical-most cell layers of the limbus and cornea of both the age-matched unwounded synd1ko and the wounded wild-type mice. However, in the wounded synd1ko corneas, ZO-1 staining was diffuse and more wide spread. The failure of ZO-1 to repolarize properly in the synd1ko central cornea after wounding did not extend to the limbus. Tissues taken at time points ranging from 48 hours to 8 weeks confirmed defects in ZO-1 relocalization in the corneas of the

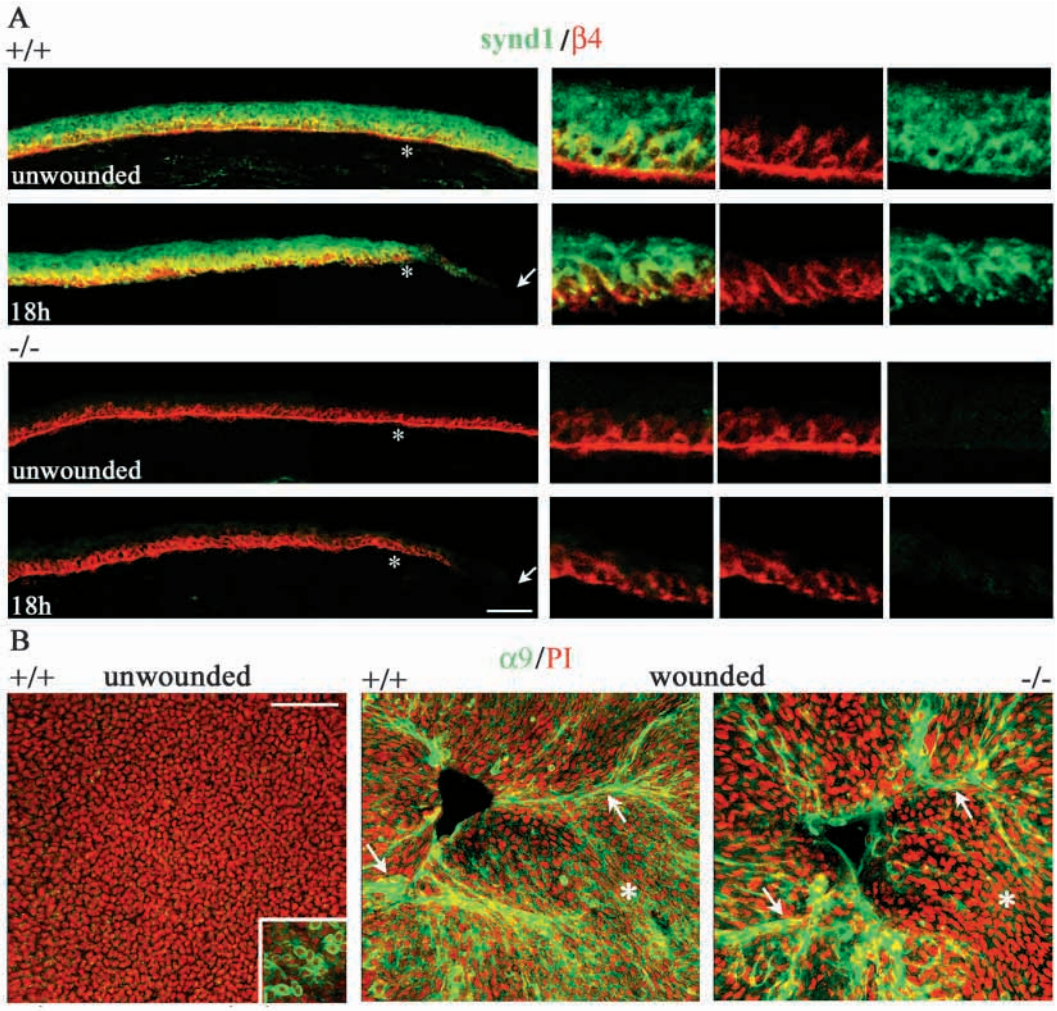

Fig. 3. Although β4 integrin localization appears normal during migration, subtle differences in the localization of α9 integrin emerge between the wild-type and synd1ko corneas immediately prior to wound closure. (A) Unwounded tissues and tissues taken at 18 hours after wounding are double-labeled to detect synd1 and β4 integrin simultaneously. Asterisks indicate the regions shown at higher magnification at the right – both as doubly and individually labeled images to allow for better determination of the regions of overlap. Arrows indicate the tip of the leading edge; migration occurs from left to right. Bar, 80 μm in lower magnification images at the left and 25 μm in higher magnification images at the right. (B) En face views of whole mounts of corneas from control or wounded mice have been treated with propidium iodide to highlight nuclei and simultaneously stained with an antibody to detect α9 integrin. α9 integrin is absent from the central corneas of unwounded wild-type animals but present at the limbal region as seen in the inset. Similar results are seen in the synd1ko mouse. When matched for the size of the remaining wound, wild-type corneas show more α9 integrin around epithelial cells close to the leading edge (asterisks) as well as at sites where seams form as advancing epithelial sheet edges merge (arrows) compared to the synd1ko corneas. Trapping of sera at the leading edge within wound opening occurs in some samples and is not specific. Bar, 150 μm.

synd1ko mice (data not shown). β4 integrin remained polarized to the basal aspect of the corneal epithelial basal cells in the wounded synd1ko mice.

The mislocalization of ZO-1 to multiple cell layers after wounding in synd1ko corneas reflects a persistent loss of tight junctions in these tissues. To determine whether this was the case, the barrier function in these tissues was assessed using a biotin penetration assay. Typical data obtained from mice 4 weeks after wounding indicate that, despite the diffuse localization of ZO-1, the barrier function was intact, and biotin had not penetrated the corneal epithelium of the synd1ko mice (Fig. 4B).

Cell proliferation defects and altered integrin expression were also observed during the healing of cutaneous wounds in the synd1ko mouse

To determine whether the synd1ko mice would also show defects in the repair of skin wounds, we first made 3 mm full-thickness skin wounds on the backs of synd1ko animals and compared healing to that of wild-type animals. Typical histological data for 5 and 9 days are shown in Fig. 5. Although no differences in the rate of wound closure could be observed before day 5, pronounced hypoplasia of the epithelial tissues within the wound bed of the synd1ko mice was seen, which persisted 9 days after wounding. The adherent palisaded layer of epithelial cells observed in the wild-type mouse skin 9 days after wounding was absent from the synd1ko mouse wound bed. The synd1ko epidermis was thin, and basal cells remained flattened and did not regain their normal columnar morphology. No differences in the expression of α-smooth-muscle actin expression in cells in the healing dermis were observed at any

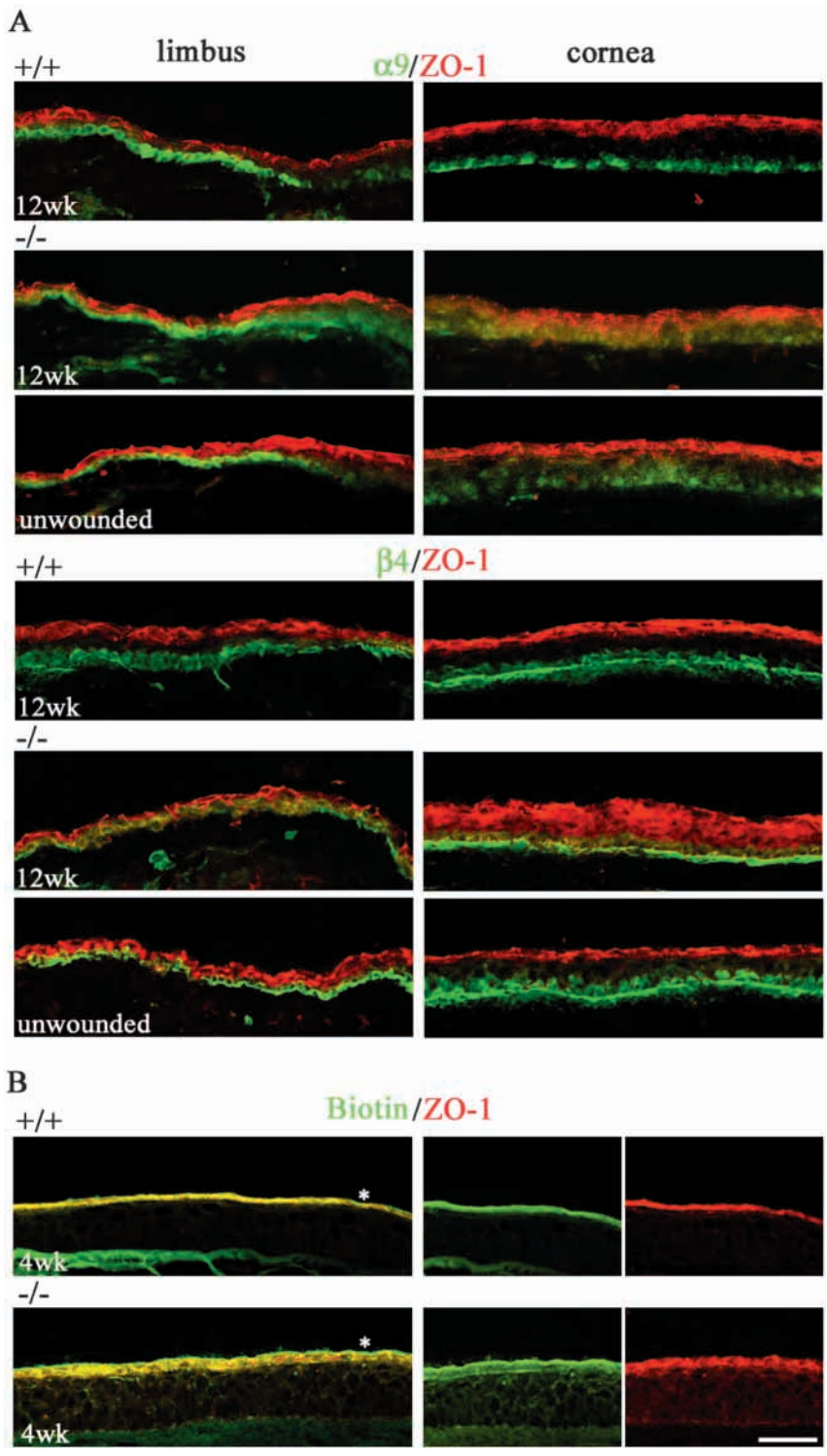

Fig. 4. Tight junctions are functional after wounding in the synd1ko mouse cornea despite the persistent failure of ZO-1 to relocalize exclusively to the apical-most cell layers in the wounded synd1ko corneas. (A) Immunofluorescence microscopy was performed to colocalize ZO-1 and α9 integrin, and ZO-1 and β4 integrin at 12 weeks after wounding in wild-type and synd1ko tissues. Age-matched unwounded synd1ko corneas were also analyzed. For all corneas shown, the limbal images are oriented with their conjunctiva to the left and their central cornea to the right. The central cornea of a wild-type mouse 12 weeks after wounding and the unwounded, age-matched, synd1ko mouse cornea at 5 months of age show polarized localization of ZO-1. However, in both of the synd1ko corneas shown 12 weeks after wounding, ZO-1 can still be seen at non-apical cell layers. α9 integrin is upregulated in response to aging in wild-type and synd1ko corneal epithelial basal cells, and this occurs with or without wounding. β4 integrin is present at the basal cell basement membrane zone in the central cornea in both unwounded and wounded wild-type and synd1ko mice. Bar, 75 μm. (B) Biotin penetration was assayed in wild-type and synd1ko corneas 4 weeks after wounding as an indication of tight junction integrity. Biotin was detected with rhodamin-avidin, and sections were simultaneously stained for ZO-1 using a goat anti-rat secondary antibody conjugated with Alexa 488. To facilitate comparison with the results presented for ZO-1 in A, Adobe Photoshop was used to invert the colors of the rhodamin-avidin to green and the Alexa-488 to red. In both wild-type and synd1ko corneas, biotin did not penetrate past ZO-1-positive cell layers, indicating that tight junctions were functional in the synd1ko corneas. Bar, 75 μm.

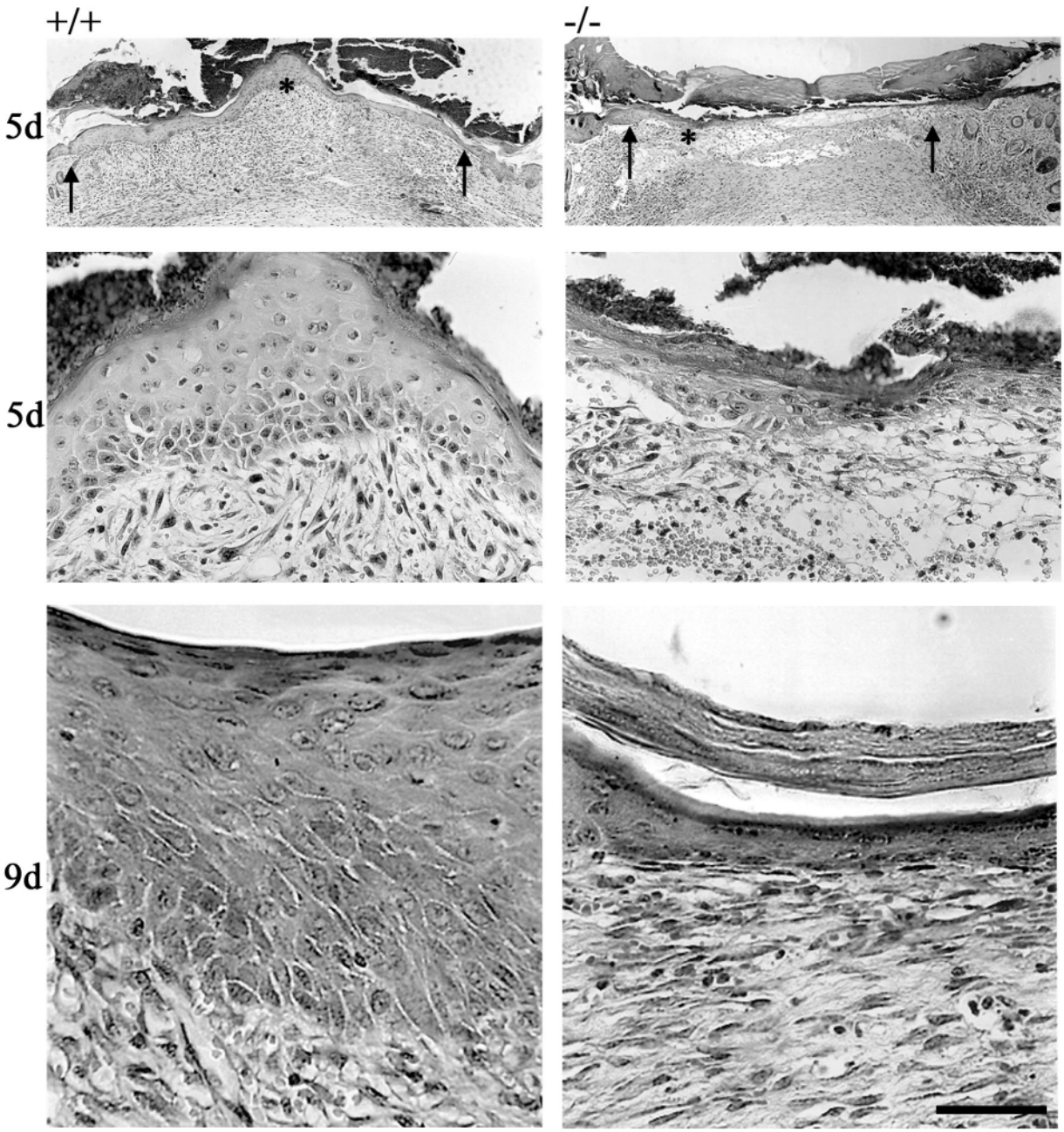

Fig. 5. Synd1ko mice show delayed re-epithelialization of full-thickness cutaneous wounds. Histology performed on fixed tissues shows that as soon as 5 days (d) after wounding, signs of defective re-epithelialization are detected in the synd1ko mice compared to wildtype. Low magnification shows wound margins 5 days after wounding, and high magnification shows the poor overall morphology of the synd1ko tissue compared with wild-type at 5, 7 and 9 days after wounding. Bar, 300 μm in the lower magnification image at day 5, bar, 50 μm in images at days 5 and 7, and bar, 25 μm in the images at day 9.

time point after wounding, and wound contraction appeared normal (data not shown). These data show that while re-epithelialization took place, restratification of closed wounds was defective in the synd1ko skin.

The above results show that poor healing after corneal and skin wounding in the synd1ko mouse is associated with hypoplasia. To assess cell proliferation and integrin expression after skin wounding, we focused our efforts on a dermabrasion rather than a full-thickness skin wound model. The rationale for changing wound healing models was to focus our attention on epithelial cell proliferation rather than migration. We found that dermabraded skin healed more slowly in the synd1ko mice, at both 2 and 5 days after wounding. In addition, synd1ko dermabrasions appeared deeper and tissues more inflamed than those of wild-type controls (Fig. 6A). Cell proliferation was assessed using BrdU, and epidermal keratinocytes from the synd1ko mice were found to proliferate at a significantly (P<0.05) higher rate prior to dermabrasion (Fig. 6B). At 2 days after wounding, there was only a slight increase in cell proliferation in the synd1ko skin cells, whereas, in the wt skin,

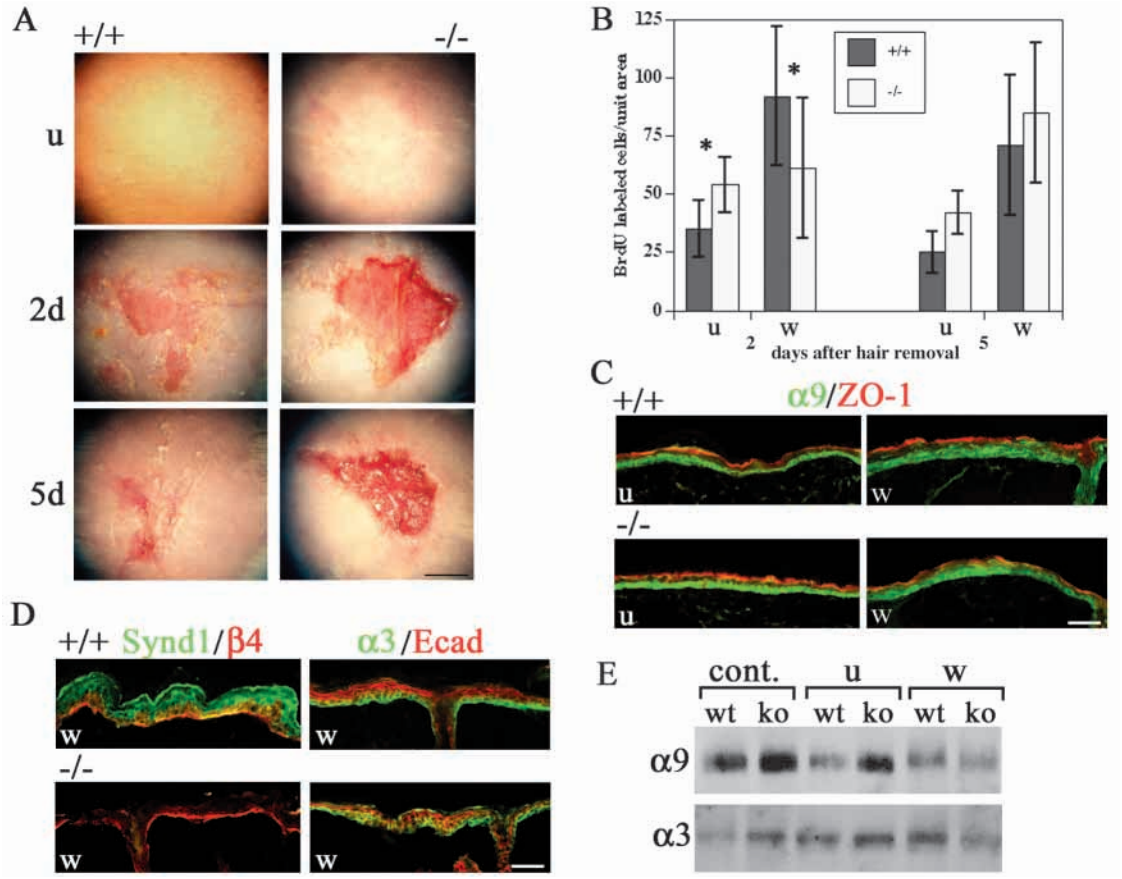

Fig. 6. Cell proliferation and integrin expression are altered in syndko mice during wound healing in response to dermabrasion. (A) Dermabrasion was performed on wild-type and synd1ko mouse back skin after removal of hair; and mice were sacrificed 2 and 5 days after hair removal. Synd1ko mouse have deeper and more inflamed wounds at both 2 and 5 days compared with the wildtype. (B) Cell proliferation was analyzed in unwounded mouse back skin from which hair had been removed 2 or 5 days previously and in dermabraded mouse skin at 2 and 5 days. Although the variation among both individual mice and within the same mouse after wounding is substantial, analyses of over 85 visual fields per sample for 2 days and over 30 visual fields for the 5-day samples yield data that are significant (P>0.05) at both 2 and 5 days by the unpaired t-test. Further, unwounded synd1ko and wild-type skin have significantly different cell proliferation rates at both 2 and 5 days after hair removal. (C) Colocalization of α9 integrin and ZO-1 indicates that unwounded skin from which hair had been removed 2 days previously has a normal distribution of ZO-1. Both wild-type and synd1ko mouse back skin show basal cell localization for α9 integrin. This distribution is similar to that observed in control skin taken from the lip, as shown in Fig. 1D. 2 days after dermabrasion, there is an increase in the number of cell layers expressing α9 integrin in the wild-type skin. The increase is less dramatic in the wounded skin of synd1ko mice. In both wild-type and synd1ko skin, ZO-1 localization over the involved skin areas is discontinuous. (D) Colocalization of β4 integrin with synd1, and α3 integrin with E-cadherin, is shown in wounded skin 2 days after dermabrasion in wild-type and synd1ko mice. There are no differences in the localization of β4 integrin, and synd1 is not present in the synd1ko tissues. α3 integrin and E-cadherin are also not differentially affected by wounding in synd1ko mice. Bar in C and D, 75 μm. (E) Immunoblots of skin tissue extracts from unwounded and dermabraded mouse skin show differences in integrin expression after wounding. Samples were normalized on the basis of their protein concentration; tissues were extracted from two mice per variable, and dermabrasion repeated twice. cont., extracts from tissues immediately after sacrifice and removal of hair; u, extracts from tissues from which hair had been removed 2 days prior to sacrifice; w, extracts from tissues from animals that had been wounded 2 days prior to sacrifice.

cell proliferation increased over three-fold. These significant differences in cell proliferation between wt and synd1ko skin persisted at 5 days after wounding.

To determine whether any differences in integrin, E-cadherin or ZO-1 localization occurred after dermabrasion in synd1ko mouse skin, tissues taken from unwounded and wounded skin 2 days after dermabrasion were used in colocalization studies (Fig. 6C,D). As had occurred after wounding in both wild-type and synd1ko corneas, α9 integrin localization increased in the keratinocytes after dermabrasion. Although it was restricted to the basal cell layer in unwounded epidermis, α9 integrin was also found in multiple cell layers of healing wild-type epidermis. In the synd1ko skin, there was also an increase in localization of α9 integrin adjacent to the involved skin, but it appeared to be more modest, affecting fewer cell layers. This result was consistent with the results observed immediately prior to wound closure in the cornea, where there also appeared to be less α9 integrin localization after wounding in the synd1ko than in the wild-type tissues (Fig. 3B). Furthermore, there were no changes observed in either α3 integrin or E-cadherin localization after dermabrasion. Similarly, β4 integrin remained localized to the basal-most cell membrane adjacent

to the basement membrane, and we saw no evidence of increased localization of β4 integrin in either wild-type or synd1ko skin after dermabrasion.

To confirm biochemical changes in integrin expression in wild-type and synd1ko mouse skin in response to dermabrasion, analyses of integrin expression were conducted in wild-type and synd1ko wounded and unwounded full-thickness skin tissues using immunoblots (Fig. 6E). The relative expression levels of α9 and α3 integrins were compared in protein extracts obtained from three different variables. Proteins were extracted from the control back skin (c), skin from which hair had been removed 2 days before but had not been dermabraded (u), and involved skin dermabraded 2 days previously (w). For samples that had been dermabraded (w), extracted tissues included a 2 mm region surrounding the involved wound bed. Data show that α3 and α9 integrins were present in higher amounts in synd1ko skin regardless of whether or not it had been subjected to hair removal 2 days prior to sacrifice. Hair removal alone stimulated α3 integrin expression in both wild-type and synd1ko skin but decreased α9 expression. At 2 days after wounding, there was no increase in either α3 or α9 integrin expression observed in extracts from the involved skin. Although confocal microscopy does not show any difference in integrin expression and localization in the skin of the synd1ko and wild-type mice (Fig. 1D), these biochemical studies suggest that expression of some integrins is enhanced in the absence of syndecan-1. After dermabrasion, confocal microscopy data show increased localization of α9 integrin in both wild-type and, to a lesser extent, in synd1ko keratinocytes adjacent to the involved wound bed (Fig. 6C). The immunoblots used whole skin extracts. After dermabrasion, degeneration of the epidermis (Fig. 6A) results in lower levels of epithelial proteins overall in wounded tissues and probably masked differences in integrin expression in the skin next to the wound site. Thus, although the immunoblot data do not provide direct support for enhanced expression of α9 integrin protein during healing, they do show that integrin expression within skin is altered in the absence of syndecan-1.

Discussion

In this study, we demonstrate that there is a defect in healing in both corneal epithelial and cutaneous wounds in the synd1ko mouse. In the cornea, this defect appears to result from both delayed re-epithelialization and failed activation of cell proliferation after wounding. mRNA profiles of wounded and unwounded corneal epithelial cells confirm differences in mRNAs between wild-type and synd1ko mice both before and after wounding. In the skin, we confirm delayed healing using a full-thickness skin wound-healing model. Although no differences in the migration rate could be observed after full-thickness skin wounding in the synd1ko mice, wounds did show a failure to restratify, and wounded areas remained thin and poorly differentiated. Using a dermabrasion model to induce epithelial cell proliferation, we went on to demonstrate that cell proliferation defects also exist in the skin prior to and after wounding. Further, after wounding in both cornea and skin, the synd1ko tissues expressed less α9 integrin than was observed in wild-type mice, although other cell adhesion molecules appeared to be expressed at similar levels compared to tissues from wild-type mice. These studies suggest roles for the synd1 HSPG in regulation of both gene transcription in quiescent keratinocytes and in keratinocyte activation after wounding. Differences in integrin expression, although subtle, suggest defective integrin function in the absence of synd1. Taken together, our data confirm essential roles for the syndecan family of heparan sulfate proteoglycans in wound healing and in the regulation of cell proliferation in epithelial tissues.

Surprisingly, there were no differences detected in the localization of cytoskeletal proteins, including filamentous actin, vinculin, talin and α-actinin in synd1ko corneas. Both α3β1 and α6β4 laminin-binding integrins have been implicated in mediating epithelial cell migration in response to injury (Belkin and Stepp, 2000), and their ligand, laminin-5, and its cleavage play a role in facilitating stable or transient integrin-mediated cellular attachment (Gianelli et al., 1997; Goldfinger et al., 1998; Goldfinger et al., 1999). α6β4 protein expression increases in wild-type mice after corneal scrape wounding (Stepp et al., 1997), and in this study, we show a comparable increase in the wounded synd1ko mouse corneas. However, after induction of cell proliferation in skin by dermabrasion, β4 integrin localization was unaltered in the wild-type and synd1ko basal cells, suggesting that the enhanced expression of α6β4 after full thickness skin wounding maybe related more to the disassembly of hemidesmosomes and induction of cell migration than to induction of cell proliferation.

Although we demonstrated cell migration delays in the synd1ko corneal keratinocytes, full-thickness skin wounds did not show delayed migration; however, it is possible that the complexity of wound healing after full-thickness skin wounding masked the difference in keratinocyte migration. Re-epithelialization after a full-thickness skin wounding involves epithelial cell migration as well as wound contraction and the growth of new blood vessels into the wound site. Keratinocyte proliferation and differentiation are known to be subject to regulation by paracrine secretion of factors by both keratinocytes and dermal fibroblasts (Werner and Smola, 2001). Synd1 expression is normally upregulated in both the dermis and the epithelium after skin wounding. Defects in both stromal cells and keratinocytes could contribute to the overall wound healing phenotype observed in the synd1ko mice. The use of the corneal model for studies of re-epithelialization eliminates several extrinsic factors present in the skin-healing model that complicate assessment of migration rates, since it was developed to minimize activation of stromal fibroblasts and allow cells to migrate over a native basement membrane zone in the absence of induction of neovascularization. However, even in the corneal model, defects in stromal fibroblast secretion of cytokines could contribute to the healing phenotype observed.

A dermabrasion wound model was used as it is less invasive than a full-thickness wound model and involves primarily keratinocytes, thus leaving the basal cell–basement-membrane hemidesmosome interaction intact. Moreover, dermal response following dermabrasion is minimal; therefore, this type of wound is ideal for assessing keratinocyte cell proliferation. To perform dermabrasion, the hair overlying the area to be wounded was removed, inducing quiescent hair follicles to enter the active growth stage, anagen. Thus, proliferation of cells from the hair follicles is a contributing

factor to the responses to dermabrasion we observed. Although only BrdU-labeled interfolicular keratinocytes were counted for cell proliferation studies, differences in hair follicle regrowth in the synd1ko mouse might contribute to the healing phenotype. Given the epithelial cell migration and proliferation defects revealed in our studies, the known roles played by EGFR and α6β4 in mediating both migration and proliferation in keratinocytes (Mainiero et al., 1997; Murgia et al., 1998; Dans et al., 2001; Mariotti at al., 2001) and the ability of syndecans to function as co-receptors with integrins for growth factors and matrix proteins (Couchman and Woods, 1999; Saoncella et al., 1999; Woods, 2001), it seems likely that altered signaling via the α6β4 integrin is responsible for some of the phenotypic properties displayed by synd1ko keratinocytes after wounding.

α9 integrin localization is reduced in the wounded synd1ko corneal and epidermal keratinocytes compared with wounded wild-type cells. Immunoblots from wild-type dermabraded skin show a reduction in α9 integrin in response to hair removal as well as no change or a slight increase in the amount of α9 integrin after wounding. The immunoblots also showed that in the synd1ko skin, α9 decreases with hair removal and during healing. α3 integrin is increased in both the wild-type and synd1ko cells after hair removal, and wounding causes no change in α3 integrin in the wild-type cells and a slight reduction in the synd1ko cells. The transient increase in α9 integrin localization immediately prior to wound closure observed using wounded corneal whole mounts extends results we first reported several years ago (Stepp and Zhu, 1997). In closed corneal wounds of wild-type mice 24 hours after wounding, we reported a transient increase in α9 integrin mRNA and protein in the corneal basal cells but no increase in α9 integrin 18 or 48 hours after wounding. Using whole mounts, we show, in the current study, that the increased expression of α9 integrin does not occur after migration is completed but immediately prior to its completion.

The distinct localization of the α9 integrin within corneal keratinocytes just prior to wound closure suggests that it functions to seal off the edges of the advancing wound margins. The ligand(s) recognized by keratinocyte α9 integrin remain unknown. Known ligands for α9 integrin include tenascin-C (Yokosaki et al., 1994), osteopontin (Yokosaki et al., 1999), VCAM-1 (Taooka et al., 1999), von Willibrand factor (Takahashi et al., 2000), tissue transglutaminase (Takahashi et al., 2000), blood coagulation factor XIII (Takahashi et al., 2000), L1-CAM (Silletti et al., 2000) and ADAMs-12 and -15 (Eto et al., 2000). The most recently characterized ligand is perhaps the most intriguing, the EIIIA segment of fibronectin (FN); this alternatively spliced region of FN was previously thought to be recognized only by α4 integrin (Liao et al., 2002). α4 and α9 integrins are close homologs, sharing 39% amino-acid identity, and among the reported α9 ligands, all except tenascin-C also interact with α4 integrin. Numerous studies have reported the upregulation of EIIIA after wounding in skin (ffrench-Constant et al., 1989) and cornea (Cai et al., 1993; Vitale et al., 1994; Nickeleit, 1996). However, given that α4 integrin is not expressed by skin and corneal keratinocytes, the significance of FN to corneal wound healing remains unclear (Gipson et al., 1993).

If α9 integrin can be shown to mediate cell migration after wounding by interacting with the EIIIA domain of FN, then the function of FN alternative splicing in skin and corneal wound healing might be revealed. Further, the reduced localization of α9 integrin in the synd1ko corneas prior to closure and in skin after dermabrasion may be contributing to the healing delay. It is also tempting to suggest that the interaction between α9 integrin and ADAMs might be altered in the absence of synd1, given that both α9 integrin (Eto et al., 2000) and synd1 (Iba et al., 2000) can interact with ADAM-12. Unfortunately, α9 integrin expression is not maintained in cultured keratinocytes under standard conditions. This explains not only why keratinocytes have not been shown to interact with this alternatively spliced FN isoform but also why the ligand(s) for this integrin within epithelial tissues remain unknown.

It was initially surprising that synd1ko mice were viable and had no obvious phenotype. Yet our studies demonstrated that they are defective in cutaneous and corneal wound healing. Our data add to those reporting defective leukocyte adhesion and increased angiogenesis in the synd1ko mice (Gotte et al., 2002). Echtermeyer and colleagues deleted the gene encoding synd4 in mice and also observed a cutaneous wound-healing defect (Echtermeyer et al., 2001). Furthermore, these synd4ko mice showed signs of delayed closure and impaired angiogenesis, with fibroblasts derived from the synd4ko mice showing slower than normal migration rates as well as poorly forming focal adhesions (Ishiguro et al., 2000). In the synd1ko mouse, the keratinocytes fail not only to activate cell proliferation in response to wounding but also to revert completely back to normal after migration is complete.

Improved primary epithelial cell culture models for both wild-type and synd1ko keratinocytes that maintain α9 integrin expression would be a great aid in determining the role played by α9 integrin in mediating the healing defects in the synd1ko mouse. In addition, the generation of mice lacking multiple syndecan family members will allow for the exact determination of how each of the syndecan HSPGs interacts developmentally and within tissues to maintain appropriate tissue- and organ-specific functions. Delayed healing is a hallmark of aging, so a better understanding of the functions of the molecules that mediate proper wound healing will allow us to develop better treatments for those who suffer the consequences of impaired healing.

Portions of this work represent the undergraduate honors thesis of one of our co-authors (P.G.). Technical assistance was obtained from Tianging Qiu at George Washington University (GWU). Discussions held with Caroline Alexander, Ofer Reizes and James Zieske helped to clarify ideas and suggest new directions. Robyn Rufner, Director of the GWU Center for Microscopy and Image Analysis, assisted with the confocal microscopy and imaging. We were supported by grant RO1 EYO8512 and a Faculty Research and Enhancement Fund Grant from GWU Medical Center to M.A.S.; Sigma Xi Student Achievement Award to P.H.G. and R01 CA28763 to M.B.

References

Alexander, C. M., Reichsman, F., Hinkes, M. T., Lincecum, J., Becker, K. A., Cumberledge, S. and Bernfield, M. (2000). Syndecan 1 is required for Wnt-1-induced mammary tumorigenesis in mice. *Nat. Genet.* **25**, 329-332.

Belkin, A. M. and Stepp, M. A. (2000). Integrins as receptors for laminins. *Micro. Res. Tech.* **51**, 280-301.

Bernfield, M., Gotte, M., Park, P. W., Reizes, O., Fitzgerald, M. L., Lincecum, J. and Zako, M. (1999). Functions of cell surface heparan sulfate proteoglycans. *Annu. Rev. Biochem.* **68**, 729-777.

Brockstedt, U., Dobra, K., Nurminen, M. and Hjerpe, A. (2002). Immunoreactivity to cell surface syndecans in cytoplasm and nucleus: tubulin-dependent rearrangements. *Exp. Cell Res.* **274**, 235-245.

Cai, X., Foster, C. S., Liu, J. J., Kupferman, A. E., Filipec, M., Colvin, R. B. and Lee, S. J. (1993). Alternatively spliced fibronectin molecules in the wounded cornea: analysis by PCR. *Invest. Ophthalmol. Vis. Sci.* **34**, 3585-3592.

Cornelison, D. D., Filla, M. S., Stanley, H. M., Rapraeger, A. C. and Olwin, B. B. (2001). Syndecan-3 and syndecan-4 specifically mark skeletal muscle satellite cells and are implicated in satellite cell maintenance and muscle regeneration. *Dev. Biol.* **239**, 79-94.

Couchman, J. R. and Woods, A. (1999). Syndecan-4 and integrins: combinatorial signaling in cell adhesion. *J. Cell Sci.* **112**, 3415-3420.

Dans, M., Gagnoux-Palacios, L., Blaikie, P., Klein, S., Mariotti, A. and Giancotti, F. G. (2001). Tyrosine phosphorylation of the β4 integrin cytoplasmic domain mediates Shc signaling to extracellular signal-regulated kinase and antagonizes formation of hemidesmosomes. *J. Biol. Chem.* **276**, 1494-1502.

Derksen, P. W., Keehnen, R. M., Evers, L. M., van Oers, M. H., Spaargaren, M. and Pals, S. T. (2002). Cell surface proteoglycan syndecan-1 mediates hepatocyte growth factor binding and promotes Met signaling in multiple myeloma. *Blood* **99**, 1405-1410.

Dobra, K., Andang, M., Syrokou, A., Karamanos, N. K. and Hjerpe, A. (2000). Differentiation of mesothelioma cells is influenced by the expression of proteoglycans. *Exp. Cell Res.* **258**, 12-22.

Echtermeyer, F., Streit, M., Wilcox-Adelman, S., Saoncella, S., Denhez, F., Detmar, M. and Goetinck. P. (2001). Delayed wound repair and impaired angiogenesis in mice lacking syndecan-4. *J. Clin. Invest.* **107**, R9-R14.

Eto, K., Puzon-McLaughlin, W., Sheppard, D., Sehara-Fujisawa, A., Zhang, X. P. and Takada, Y. (2000). RGD-independent binding of integrin α9β1 to the ADAM-12 and -15 disintegrin domains mediates cell-cell interaction. *J. Biol. Chem.* **275**, 34922-34930.

ffrench-Constant, C., van de Water, L., Dvorak, H. F. and Hynes, R. O. (1989). Reappearance of an embryonic pattern of fibronectin splicing during wound healing in the adult rat. *J. Cell Biol.* **109**, 903-914.

Filla, M. S., Dam, P. and Rapraeger, A. C. (1998) The cell surface proteoglycan syndecan-1 mediates fibroblast growth factor-2 binding and activity. *J. Cell Physiol.* **174**, 310-321.

Fitzgerald, M. L., Wang, Z., Park, P. W., Murphy, G. and Bernfield, M. (2000). Shedding of syndecan-1 and -4 ectodomains is regulated by multiple signaling pathways and mediated by a TIMP-3-sensitive metalloproteinase. *J. Cell Biol.* **148**, 811-824.

Fujikawa, L. S., Foster, C. S., Gipson, I. K. and Colvin, R. B. (1984). Basement membrane components in healing rabbit corneal epithelial wounds: immunofluorescence and ultrastructural studies. *J. Cell Biol.* **98**, 128-138.

Fuki, I. V., Meyer, M. E. and Williams, K. J. (2000). Transmembrane and cytoplasmic domains of syndecan mediate a multi-step endocytic pathway involving detergent-insoluble membrane rafts. *Biochemical. J.* **351**, 607-612.

Giannelli, G., Falk-Marzillier, G., Schiraldi, O., Stetler-Stevenson, W. G. and Quaranta, V. (1997). Induction of cell migration by matrix metalloprotease-2 cleavage of laminin-5. *Science* **277**, 225-228.

Gipson, I. K., Kiorpes, T. C. and Brennan, S. J. (1984). Epithelial sheet movement: effects of tunicamycin on migration and glycoprotein synthesis. *Dev. Biol.* **101**, 212-220.

Gipson, I. K., Watanabe, H. and Zieske, J. D. (1993). Corneal wound healing and fibronectin. *Int. Ophthalmol. Clinics.* **33**, 149-163.

Goldfinger, L. E., Stack, M. S. and Jones, J. C. (1998). Processing of laminin-5 and its functional consequences: role of plasmin and tissue-type plasminogen activator. *J. Cell Biol.* **141**, 255-265.

Goldfinger, L. E., Hopkinson, S. B., deHart, G. W., Collawn, S., Couchman, J. R. and Jones, J. C. (1999). The α3 laminin subunit, α6β4 and α3β1 integrin coordinately regulate wound healing in cultured epithelial cells and in the skin. *J. Cell Sci.* **112**, 2615-2629.

Gotte, M., Joussen, A. M., Klein, C., Andre, P., Wagner, D. D., Hinkes, M. T., Kirchhof, B., Adamis, A. P. and Bernfield, M. (2002). Role of syndecan-1 in leukocyte-endothelial interactions in the ocular vasculature. *Invest. Ophthalmol. Vis. Sci.* **43**, 1135-1141.

Grootjans, J. J., Reekmans, G., Ceulemans, H. and David, G. (2000). Syntenin-syndecan binding requires syndecan-synteny and the cooperation of both PDZ domains of syntenin. *J. Biol. Chem.* **275**, 19933-19941.

Grootjans, J. J., Zimmermann, P., Reekmans, G., Smets, A., Degeest, G., Durr, J. and David, G. (1997). Syntenin, a PDZ protein that binds syndecan cytoplasmic domains. *Proc. Natl. Acad. Sci. USA* **94**, 13683-13688.

Hertle, M. D., Kubler, M. D., Leigh, I. M. and Watt, F. M. (1992). Aberrant integrin expression during epidermal wound healing and in psoriatic epidermis. *J. Clin. Invest.* **89**, 1892-1901.

Hinkes, M. T., Goldberger, O. A., Neumann, P. E., Kokenyesi, R. and Bernfield, M. (1993). Organization and promoter activity of the mouse syndecan-1 gene. *J. Biol. Chem.* **268**, 11440-11448.

Hsueh, Y. P., Wang, T. F., Yang, F. C. and Sheng, M. (2000). Nuclear translocation and transcription regulation by the membrane-associated guanylate kinase CASK/LIN-2. *Nature* **404**, 298-302.

Hsueh, Y. P. and Sheng, M. (1999). Regulated expression and subcellular localization of syndecan heparan sulfate proteoglycans and the syndecan-binding protein CASK/LIN-2 during rat brain development. *J. Neurosci.* **19**, 7415-7425.

Iba, K., Albrechtsen, R., Gilpin, B., Frohlich, C., Loechel, F., Zolkiewska, A., Ishiguro, K., Kojima, T., Liu, W., Langford, J. K. et al. (2000). The cysteine-rich domain of human ADAM 12 supports cell adhesion through syndecans and triggers signaling events that lead to beta1 integrin-dependent cell spreading. *J. Cell Biol.* **149**, 1143-1156.

Ishiguro, K., Kadomatsu, K., Kojima, T., Muramatsu, H., Nakamura, E., Ito, M., Nagasaka, T., Kobayashi, H., Kusugami, K., Saito, H. et al. (2000). Syndecan-4 deficiency impairs the fetal vessels in the placental labyrinth. *Dev. Dyn.* **219**, 539-544.

Kainulainen, T., Hakkinen, L., Hamidi, S., Larjava, K., Kallioinen, M., Peltonen, J., Salo, T., Larjava, H. and Oikarinen, A. (1998). Laminin-5 expression is independent of the injury and the microenvironment during reepithelialization of wounds. *J. Histochem. Cytochem.* **46**, 353-360.

Kainulainen, V., Wang, H., Schick, C. and Bernfield, M. (1998). Syndecans, heparan sulfate proteoglycans, maintain the proteolytic balance of acute wound fluids. *J. Biol. Chem.* **273**, 11563-11569.

Kim, C. W., Goldberger, O. A., Gallo, R. L. and Bernfield, M. (1994). Members of the syndecan family of heparan sulfate proteoglycans are expressed in distinct cell-, tissue-, and development-specific patterns. *Mol. Biol. Cell* **5**, 797-805.

Kusano, Y., Oguri, K., Nagayasu, Y., Munesue, S., Ishihara, M., Saiki, I., Yonekura, H., Yamamoto, H. and Okayama, M. (2000). Participation of syndecan 2 in the induction of stress fiber formation in cooperation with integrin α5β1: structural characteristics of heparan sulfate chains with avidity to COOH-terminal heparin-binding domain of fibronectin. *Exp. Cell Res.* **256**, 434-444.

Laird, P. W., Zijderveld, A., Linders, K., Rudnicki, M. A., Jaenisch, R. and Berns, A. (1991). Simplified mammalian DNA isolation procedure. *Nucleic Acids Res.* **19**, 4293.

Li, E., Bestor, T. H. and Jaenisch, R. (1992). Targeted mutation of the DNA methyltransferase gene results in embryonic lethality. *Cell* **69**, 915-926.

Liao, Y. F., Gotwals, P. J., Koteliansky, V. E., Sheppard, D. and van de Water, L. (2002). The EIIIA segment of fibronectin is a ligand for integrins α9β1 and α4β1 providing a novel mechanism for regulating cell adhesion by alternative splicing. *J. Biol. Chem.* **277**, 14467-14474.

Mainiero, F., Murgia, C., Wary, K. K., Curatola, A. M., Pepe, A., Blumemberg, M., Westwick, J. K., Der, C. J. and Giancotti, F. G. (1997). The coupling of α6β4 integrin to Ras-MAP kinase pathways mediated by Shc controls keratinocyte proliferation. *EMBO J.* **16**, 2365-2375.

Mariotti, A., Kedeshian, P. A., Dans, M., Curatola, A. M., Gagnoux-Palacios, L. and Giancotti, F. G. (2001). EGF-R signaling through Fyn kinase disrupts the function of integrin α6β4 at hemidesmosomes: role in epithelial cell migration and carcinoma invasion. *J. Cell Biol.* **155**, 447-458.

Murgia, C., Blaikie, P., Kim, N., Dans, M., Petrie, H. T. and Giancotti, F. G. (1998). Cell cycle and adhesion defects in mice carrying a targeted deletion of the integrin β4 cytoplasmic domain. *EMBO J.* **17**, 3940-3951

Nickeleit, V., Kaufman, A. H., Zagachin, L., Dutt, J. E., Foster, C. S. and Colvin, R. B. (1996). Healing corneas express embryonic fibronectin isoforms in the epithelium, subepithelial stroma, and endothelium. *Am. J. Pathol.* **149**, 549-558.

Park, P. W., Pier, G. B., Preston, M. J., Goldberger, O. A., Fitzgerald, M. L. and Bernfield, M. (2000a). Syndecan-1 shedding is enhanced by LasA, a secreted virulence factor of *Pseudomonas aeruginosa*. *J. Biol. Chem.* **275**, 3057-3064.

Park, P. W., Reizes, O. and Bernfield, M. (2000b). Cell surface heparan sulfate proteoglycans: selective regulators of ligand-receptor encounters. *J. Biol. Chem.* **275**, 29923-29926.

Park, P. W., Pier, G. B., Hinkes, M. T. and Bernfield, M. (2001).

Exploitation of syndecan-1 shedding by *Pseudomonas aeruginosa* enhances virulence. *Nature* **411**, 98-102.

Perrimon, N. and Bernfield, M. (2000). Specificities of heparan sulphate proteoglycans in developmental processes. *Nature* **404**, 725-728.

Perrimon, N. and Bernfield, M. (2001). Cellular functions of proteoglycans – an overview. *Semin. Cell Dev. Biol.* **12**, 65-67.

Rapraeger, A. C. (2000). Syndecan-regulated receptor signaling. *J. Cell Biol.* **149**, 995-998.

Rapraeger, A. C. (2001). Molecular interactions of syndecans during development. *Semin. Cell Dev. Biol.* **12**, 107-116.

Saoncella, S., Echtermeyer, F., Denhez, F., Nowlen, J. K., Mosher, D. F., Robinson, S. D., Hynes, R. O. and Goetinck, P. F. (1999). Syndecan-4 signals cooperatively with integrins in a Rho-dependent manner in the assembly of focal adhesions and actin stress fibers. *Proc. Natl. Acad. Sci. USA* **96**, 2805-2810.

Silletti, S., Mei, F., Sheppard, D. and Montgomery, A. M. (2000). Plasmin-sensitive dibasic sequences in the third fibronectin-like domain of L1-cell adhesion molecule (CAM) facilitate homomultimerization and concomitant integrin recruitment. *J. Cell Biol.* **149**, 1485-1502.

Sta. Iglesia, D. D., Gala, P. H., Qiu, T. and Stepp, M. A. (2000). Integrin expression during epithelial migration and restratification in the tenascin-C-deficient mouse cornea. *J. Histochem. Cytochem.* **48**, 363-376.

Stepp, M. A. and Zhu, L. (1997). Upregulation of α9 integrin and tenascin during epithelial regeneration after debridement in the cornea. *J. Histochem. Cytochem.* **45**, 189-201.

Stepp, M. A., Zhu, L. and Cranfill, R. (1996). Changes in β4 integrin expression and localization in vivo in response to corneal epithelial injury. *Invest. Ophthalmol. Vis. Sci.* **37**, 1593-1601.

Takahashi, H., Isobe, T., Horibe, S., Takagi, J., Yokosaki, Y., Sheppard, D. and Saito, Y. (2000). Tissue transglutaminase, coagulation factor XIII, and the pro-polypeptide of von Willebrand factor are all ligands for the integrins α9β1 and α4β1. *J. Biol. Chem.* **275**, 23589-23595.

Taooka, Y., Chen, J., Yednock, T. and Sheppard, D. (1999). The integrin α9β1 mediates adhesion to activated endothelial cells and transendothelial neutrophil migration through interaction with vascular cell adhesion molecule-1. *J. Cell Biol.* **145**, 413-420.

Thomas, K. R. and Capecchi, M. R. (1987). Site-directed mutagenesis by gene targeting in mouse embryo-derived stem cells. *Cell* **51**, 503-512.

Vitale, A. T., Pedroza-Seres, M., Arrunategui-Correa, V., Lee, S. J., DiMeo, S., Foster, C. S. and Colvin, R. B. (1994). Differential expression of alternatively spliced fibronectin in normal and wounded rat corneal stroma versus epithelium. *Invest. Ophthalmol. Vis. Sci.* **35**, 3664-3672.

Werner, S. and Smola, H. (2001). Paracrine regulation of keratinocyte proliferation and differentiation. *Trends Cell Biol.* **11**, 143-146.

Wojcik, S. M., Bundman, D. S. and Roop, D. R. (2000). Delayed wound healing in keratin 6a knockout mice. *Mol. Cell. Biol.* **20**, 5248-5255.

Woods, A. (2001). Syndecans: transmembrane modulators of adhesion and matrix assembly. *J. Clin. Invest.* **107**, 935-941.

Xu, K.-P., Li, X.-F. and Yu, F.-S. (2000). Corneal organ culture model for assessing epithelial responses to surfactants. *Toxicol. Sci.* **58**, 306-314.

Yokosaki, Y., Palmer, E. L., Prieto, A. L., Crossin, K. L., Bourdon, M. A., Pytela, R. and Sheppard, D. (1994). The integrin α9β1 mediates cell attachment to a non-RGD site in the third fibronectin type III repeat of tenascin. *J. Biol. Chem.* **269**, 26691-26696.

Yokosaki, Y., Matsuura, N., Sasaki, T., Murakami, I., Schneider, H., Higashiyama, S., Saitoh, Y., Yamakido, M., Taooka, Y. and Sheppard, D. (1999). The integrin α9β1 binds to a novel recognition sequence (SVVYGLR) in the thrombin-cleaved amino-terminal fragment of osteopontin. *J. Biol. Chem.* **274**, 36328-36334.

Zajchowski, L. D. and Robbins, S. M. (2002). Lipid rafts and little caves: Compartmentalized signalling in membrane microdomains. *Eur. J. Biochem.* **269**, 737-752.